JOURNAL OF MATERIALS SCIENCE 32 (1997) 6191–6200

Formation of a crack-free joint between Ti alloy and Al alloy by using a high-power CO_2 laser

B. MAJUMDAR, R. GALUN, A. WEISHEIT, B. L. MORDIKE
Institut für Werkstoffkunde und Werkstofftechnik, Technische Universität Clausthal, 38678 Clausthal-Zellerfeld, Germany

The present paper aims at producing a crack-free weld between a commercially available Ti alloy (Ti–6 wt% Al–4 wt% V) and a wrought Al alloy (Al–1 wt% Mg–0.9 wt% Si). Ti alloy and Al alloy with a plate thickness of 3 mm are butt welded using a 2.5 kW continuous CO_2 laser. The laser power, welding speeds and offset of the laser with respect to the joint are considered as the variable parameters. It is observed that intermetallic compounds (mainly TiAl and Ti_3Al) are formed in the fusion zone depending on the amount of Al and Ti melted by the laser. These intermetallic phases are very brittle and the solid-state cracks are formed near the Al side of the interface because of the stress developed after the solidification.

The formation of cracks is sensitive to the total Al content in the fusion zone. In order to minimize the dissolution of Al in the fusion zone and to increase the toughness of the intermetallic phases, Nb foil is added as a buffer between the Ti alloy and Al alloy workpieces. It is observed that the partially melted Nb acts as a barrier to dissolve Al in the fusion zone and facilitates a good joining condition for welding of Ti alloy with Al alloy.

1. Introduction

The joining of Ti alloy with Al alloy could have a major application in the field of aerospace and automobile industry where high strength and low weight are desirable. In the aerospace industry, a wing made of Ti alloy is required to be fastened to the aluminium fuselage [1]. Several attempts have been made to join these two materials together using various welding techniques. Osokin [2] tried to fusion weld Ti and Al (lap joint) in such a way that two different weld pools were formed where Al is joined with Ti by wetting the surface. Other methods for joining these two materials such as pressure welding [3], diffusion bonding [4] and cold welding [5] processes have been reported in the literature. In all these experiments, a thin layer of $TiAl_3$ was found at the joint line.

The melting points of Ti and Al are 1667 °C and 660 °C, respectively. This wide difference in the melting points between the two metals leads to the difficulty in joining them by conventional fusion welding processes. Moreover, the phase diagram of Ti–Al [6] shows a terminal solid solubility towards the Al side, whereas a solid solution up to about 12 at% Al can be obtained towards Ti-rich alloy. The system has very high value of negative enthalpy of mixing [7]. Therefore, depending on the composition, the intermetallic compounds, namely Ti_3Al, TiAl and $TiAl_3$, can be formed in the fusion zone during welding. As Al melts first by conventional fusion welding, Ti dissolves in it and forms mostly Al_3Ti. It has a low strength compared with the TiAl and Ti_3Al and almost no ductility up to about 620 °C [8]. Therefore, the formation of this phase is not desirable during welding.

In recent years, a high-power continuous-wave CO_2 laser has been used as a concentrated heat source for joining materials. It provides many advantages over conventional welding processes which has been discussed elsewhere [9] in detail. Recently, a laser has been used for joining materials of dissimilar grades because a wide variety of materials can be welded with a single source. Sun and Ion [10] have reviewed the advantages of joining dissimilar materials using a laser and the application of it in the appropriate processing conditions.

This paper presents the result of a detailed investigation into the development of crack-free joints between commercially available Ti alloy and Al alloy by employing a high-power CO_2 laser. Ti–6 wt% Al–4 wt% V and Al–1 wt% Mg–0.9 wt% Si alloys are considered as the potential candidates because they are already in widespread use in industry. The absorptivity of the CO_2 laser beam by Ti alloy and Al alloy [11] are such that the energy required to melt the surface of Al is high compared with that for the Ti alloy. It can be shown that the melting of Al by a CO_2 laser requires an energy of 2.1×10^4 kJ, whereas for Ti alloy it is 8.4×10^3 kJ per unit mass, although Ti has a very high melting point. Therefore, it is possible to melt Ti first using a CO_2 laser even without melting Al. This can result in the formation of Ti-rich phases in the fusion zone during welding of these two metals. In this investigation, first the result on welding experiments between Ti alloy and Al alloy will be presented in detail. It will be shown that crack-free

0022–2461

joints cannot be produced without the addition of a third material. An attempt is made to understand the occurrence of these cracks in the fusion zone. This is followed by preparing a crack-free joint using a Nb plate placed between the Ti alloy and Al alloy workpieces. It acts as a barrier to dissolve Al in the fusion zone.

2. Experimental procedure

Ti–6 wt% Al–4 wt% V and Al–1 wt% Mg–0.9 wt% Si alloys with a plate thickness of 3 mm were butt welded using a 2.5 kW continuous-wave CO_2 laser (Trumpf TLF 2500). The power was varied from 1.0 to 2.5 kW and the welding speed was varied from 500 to 2000 mm min^{-1}. Other parameters for the welding experiments were as follows: laser beam offset with respect to the joint line; post-heat treatment; pre-heating; application of lateral pressure from both sides of the sample; addition of a third material (Nb for the present case) in the form of plate and wire at the joint line. Table I gives the details of the conditions for the experiments, discussed in the present paper.

Experiments were conducted by keeping the surface of the specimen at the focal point of the laser beam (focal length, 150 mm). Helium was used as the shielding gas with a flow rate of 12 l min^{-1}. A coaxial optical device was employed to operate the welding process such that the shielding gas could flow through the same nozzle with the laser beam. In this way the beam was completely surrounded by the shielding gas. Here, a steady-state keyhole could be formed.

The microstructural characterizations were carried out in an optical microscope (Zeiss) and a scanning electron microscope (Hitachi). All samples were cut along the transverse and the cross-section. These were then polished and etched both sides (Al and Ti) carefully and individually with the etchants suitable for Al and Ti, respectively. The average compositions in the welded zone were measured with the help of energy-dispersive X-ray spectroscopy (EDS) using attachment to the scanning electron microscope. A microhardness tester (Leitz Weitzlar) and a universal testing machine (Instron) were used to measure the microhardness and tensile strength, respectively. The specimens for the tensile strength measurement were prepared by employing the laser with an incident power of 2 kW and a welding speed of 1 m min^{-1}. All dimensions of the sample were in accord with the DIN Specification 50125.

3. Results

3.1. Welding of Ti–6 wt% Al–4 wt% V and Al–1 wt% Mg–0.9 wt% Si

The main problem associated with the welding of Ti alloy and Al alloy is the crack that is formed immediately

TABLE I Details of the experimental conditions for the joining of Ti alloy and Al alloy: HT, heat treatment; PH, pre-heat treatment; AP, pressure applied

Experiment	Experimental conditions			
	Power (kW)	Welding speed (m min^{-1})	Laser offset	Other conditions
1	1.5	0.25	Middle	—
2		2.00	Ti side	HT, 400 °C, 2 h; PH, 300 °C
3	2.0	0.50	Ti side	HT, 400 °C, 8 h
4		1.00	Ti side	—
5		1.00	Ti side	HT 400 °C, 2 h; PA
6		1.00	Ti side	HT, 400 °C, 8 h
7		1.50	Ti side	—
8		1.50	Ti side	HT, 400 °C, 8 h
9		2.00	Ti side	—
10		2.00	Ti side	HT, 400 °C, 2 h; PH, 350 °C
11		2.50	Ti side	—
12		3.00	Ti side	HT, 400 °C, 2 h; PH, 320 °C
13		3.30 + 1.00	Ti side	Double pass; PA
14	2.5	2.00	Ti side	—
15		3.00	Ti side	—
16	2.8	2.00	Middle	HT, 400 °C, 2 h; PA
Joining of pure Ti alloy with Al alloy				
17	2.0	1.00	Ti side	Groove in Al plate
18	2.0	1.50	Ti side	—
Joining with Nb foil placed between Ti and Al				
19	2.0	1.00	Ti side	0.2 mm Nb
20		2.00	Ti side	0.2 mm Nb; PH, 310 °C
21	2.5	1.00	Middle	0.2 mm Nb; HT 500 °C, 2 h
22	2.0	1.00	Ti–Nb	0.45 mm Nb
Joining with Nb wire placed on the top				
23	2.0	1.00	Middle	Diameter, 0.75 mm
24	2.5	1.50	Ti side	Diameter, 0.75 mm
25	2.7	1.00	Middle	Diameter, 1.2 mm; HT, 500 °C, 2 h

after the solidification with sound during the cooling cycle. A detailed investigation is carried out to understand how these cracks are formed in the weld. This is presented below.

Fig. 1a shows a representative cross-sectional microstructure of a sample welded at a speed of 0.5 m min^{-1} and with an incident power of 2 kW. The laser offset is kept towards the Ti side. One observes a frozen convection swirl in the fusion zone that is asymmetric with respect to the joint. This convection is common in many dissimilar joints [12, 13] when a concentrated heat source is applied. This is probably

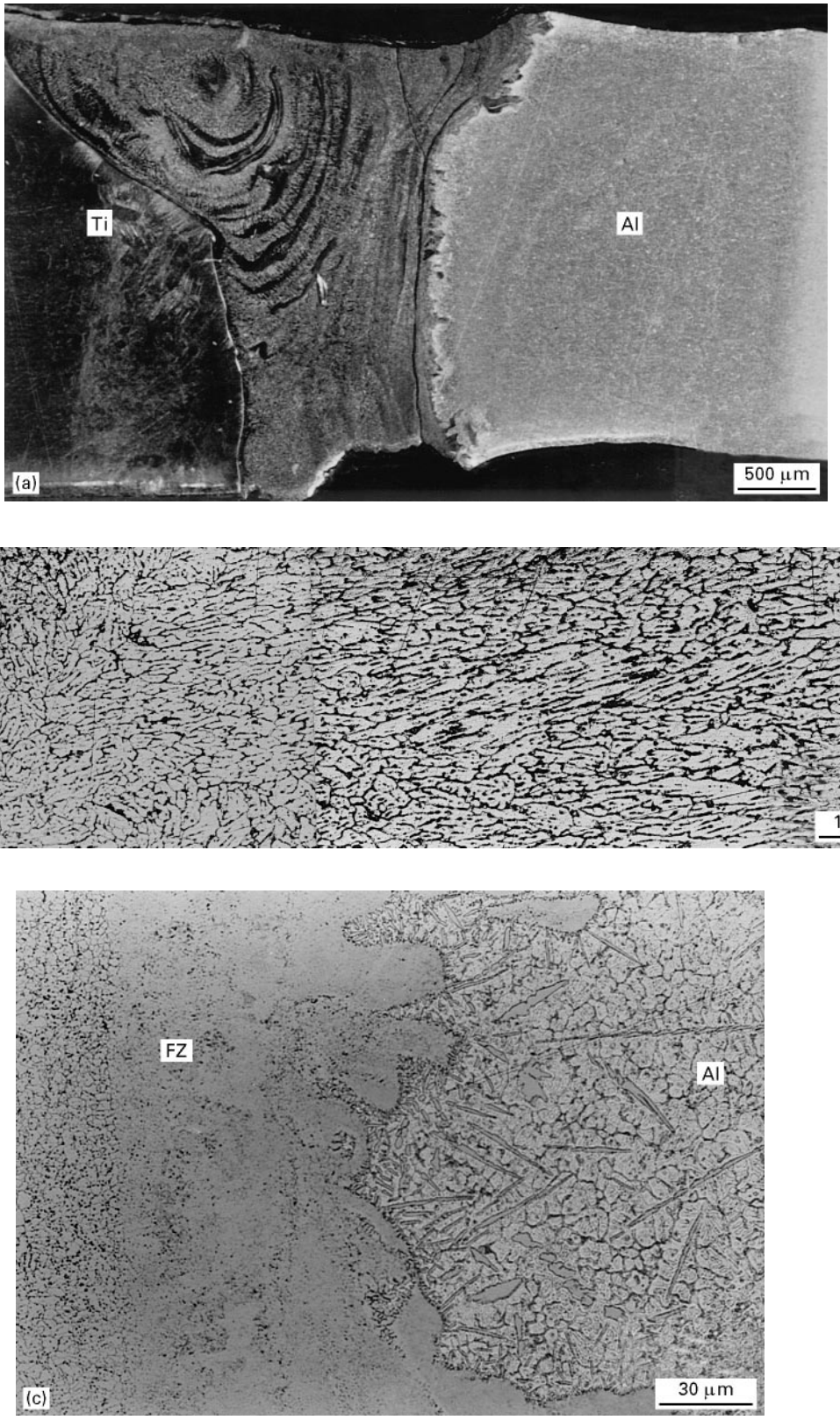

Figure 1 (a) Cross-section of the sample welded at a speed of 0.50 m min^{-1} and an incident laser power of 2.0 kW, showing the pronounced long crack in the weld near Al side interface. (b) Micrograph of the specimen welded at a speed of 0.50 m min^{-1} and an incident power of 2 kW, showing the heat-affected zone on the Al alloy side. The columnar grains indicate that the region is a resolidified zone. (c) High-magnification micrograph at the weld–Al alloy interface showing the needle-like precipitates: FZ, fusion zone.

because the very fast cooling does not allow the elements to mix properly. Long cracks originating from the surface are present in the fusion zone. It is observed in all experiments that cracks propagate only along the region close to the Al side of the interface and these are transgranular in nature. A sharp interface is observed between the Ti alloy and the fusion zone, whereas a diffuse interface exists between the fusion zone and the Al alloy side. Fig. 1b shows the region in the Al alloy adjacent to the interface. This region consists of columnar grains that are parallel to the heat transfer direction. Grains are grown from the Al alloy and become finer towards the interface owing to the increase in cooling rate. The convection is absent. Moreover, the composition analysis of this region shows a negligible Ti content. All these observations indicate that the secondary melting of Al alloy takes place by the conduction of heat and after solidification of the fusion zone. The higher-magnification microstructure of this region (Fig. 1c) shows needle-like precipitates in the Al alloy matrix near the interface for a distance of up to several microns. The EDS analysis reveals that these precipitates are predominantly Al_3Ti.

Fig. 2a represents the average concentration profiles of the laser-welded Ti alloy and Al alloy where the concentrations of Ti and Al are plotted as functions of distance from the Ti side. All concentrations are in atomic percentages. One observes that the concentrations change abruptly at the interface between Ti and the fusion zone. There exists an almost uniform composition within the weld bed. It can be seen that the Al content gradually increases towards the diffuse interface. A sharp change in the concentrations also exists between the diffuse interface and remelted Al alloy. The arrow indicates the position of the crack. The result is consistent for all experiments except for the fact that the average concentrations differ. Fig. 2b is a complementary plot which shows the concentration profiles of the fusion zone along a particular line of the joint starting from the top to bottom of the sample. A straight line is fitted and the slope of the line, drawn by regression analysis, is almost negligible. From these results, we conclude that the composition throughout the weld zone does not vary appreciably for the Ti–Al alloy system.

Fig. 3a shows the microstructure of the specimen welded at a higher speed (2.00 m min^{-1}). The laser offset is towards the Ti side. It is revealed that the crack intensity as well as the size of the resolidified zone in the Al alloy is reduced. The interface roughness is more prominent than the specimen with lower velocity. In this case the micro-cracks at the surface as well as internal cracks are developed instead of a pronounced long crack as is seen in the previous case. One also observes the presence of porosity in both the fusion and the Al remelted zone. It can be noted that the intensity of porosity decreases with the lower velocity and is almost nil for the velocity of 0.5 m min^{-1}. The corresponding concentration profile of the same sample is shown in Fig. 3b. One observes that the average composition is also reduced as compared to the previous one.

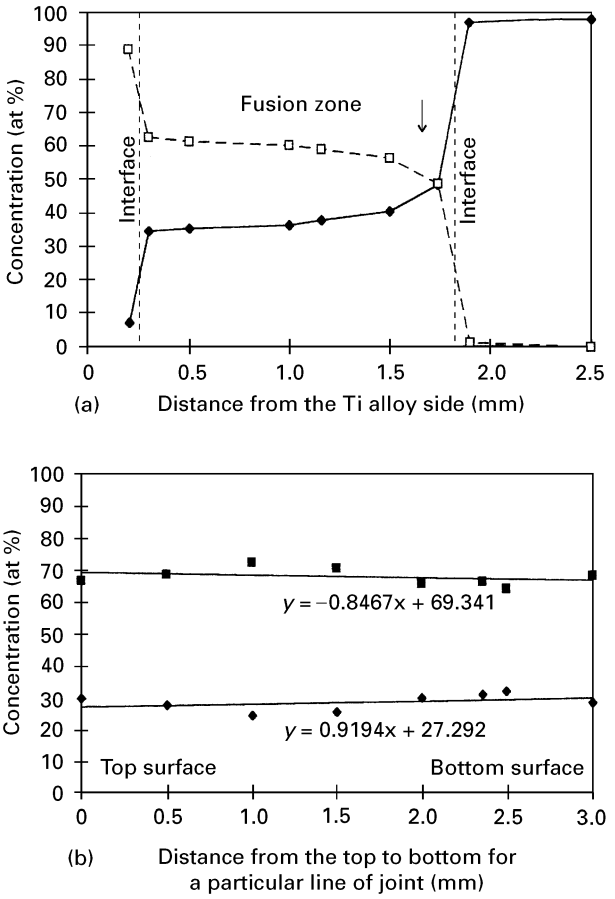

Figure 2 (a) Concentration profiles ((—◆—), Al; (– –□– –), Ti) of the specimen welded at a speed of 0.50 m min^{-1} and an incident power of 2 kW, revealing the uniform composition throughout the weld (laser offset on the Ti side). There exists a change in concentration near the crack (indicated by an arrow). (b) Concentrations of Al (◆) and Ti (■) as functions of distance from the top to bottom of the weld at a particular position. The slopes of the straight lines drawn by regression analysis are negligible.

The appearance of the longitudinal crack in the fusion zone cannot be eliminated by pre-heating the sample. Though the porosity can be reduced by pre-heating and applying lateral pressure, the more Al is dissolved in fusion zone. It is observed that the increase in Al content in the weld pool has a detrimental effect as far as crack propagation is concerned. The cracks become more pronounced when the concentration of the weld exceeds 35 at% Al. The Al content depends mainly on the laser offset with respect to the joint line. Attempts have been made to reduce the Al content in the fusion zone. It is observed in the present study that the concentration below 20 at% Al is impossible to obtain by any combination of process parameters. Too much offset of laser towards Ti side leads to the formation of the key hole only in Ti side and the mixing of the element cannot occur. It is to be noted that the quantitative estimation of the laser offset could not be evaluated in the present study. Very high velocity can lead to the incomplete melting of materials.

Fig. 4 shows the microstructure of the fusion zone-Al alloy interface for the specimen welded at a speed of

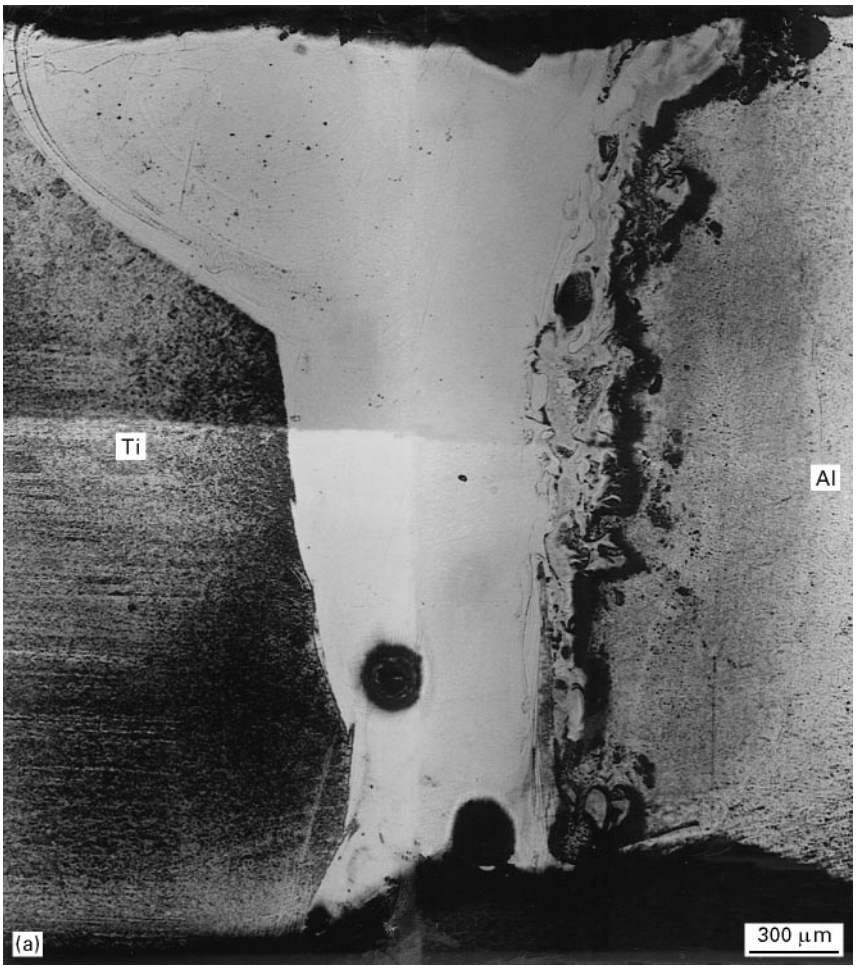

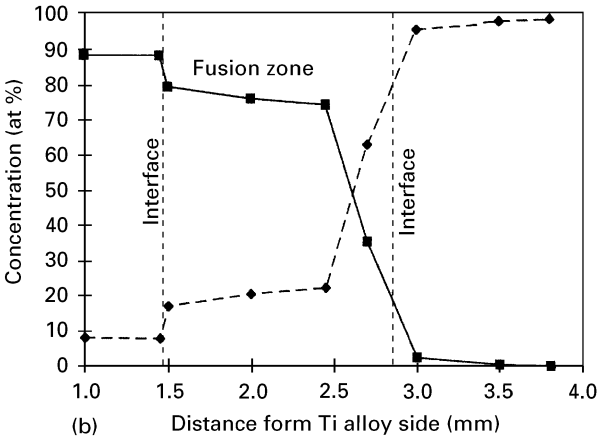

Figure 3 (a) Cross-section of the sample welded at a speed of 2.00 m min^{-1} and an incident laser power of 2.0 kW. The micrograph shows only a surface-originated microcrack instead of a long pronounced crack. (b) Concentration profiles of the same sample indicating that the average Al content in the weld is less when compared with the previous sample (laser offset on the Ti side).

1 m min^{-1} and with the laser power of 2 kW. One observes a solidification crack in the zone of resolidified Al alloy. The crack is intergranular in nature and perpendicular to the solidification direction. Porosities are also observed in the sample. The crack in this region is found occasionally and the occurrence of it could not be generalized with laser parameters used for the present study. Solidification cracks and porosity are very often found in laser welded Al alloys [14]. It is noteworthy that in this specimen, there is no longitudinal crack in the weld near the Al alloy interface. This gives an evidence that cracks in the fusion zone are formed after the solidification of Al alloys. In this case, the solidification crack acts as a sink for the relaxation of the stress in the fusion zone.

Apart from longitudinal cracks, transgranular transverse cracks are also present in the weld Fig. 5 shows an example of this crack along the transverse direction. One observes that the cracks are formed at an interval. The frequency of this type of crack is increased in the sample with high velocity condition. The preheating reduces the crack intensity.

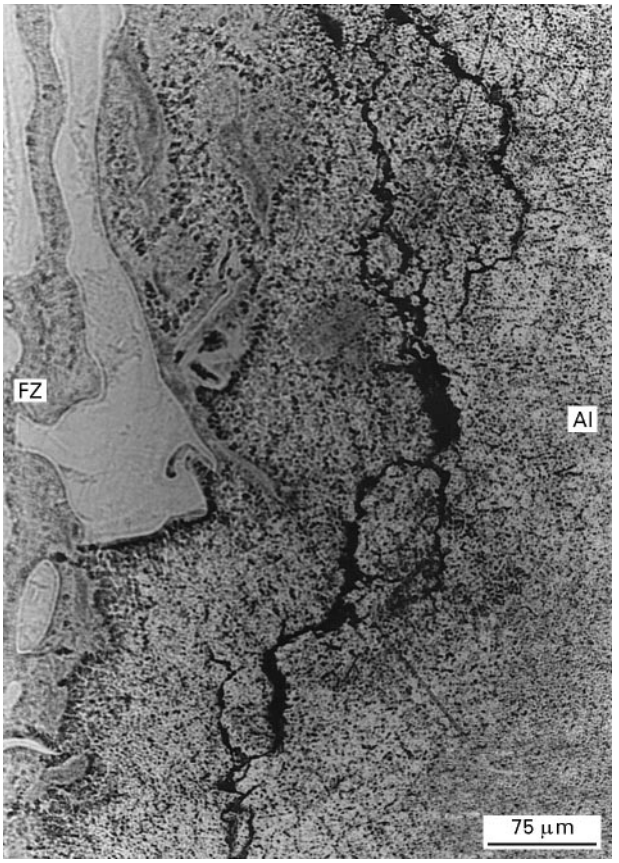

Figure 4 Cross-section of the sample welded at a speed of 1.00 m min^{-1} and a laser power of 2.0 kW, showing intergranular crack in the resolidified zone of Al alloy: FZ, fusion zone.

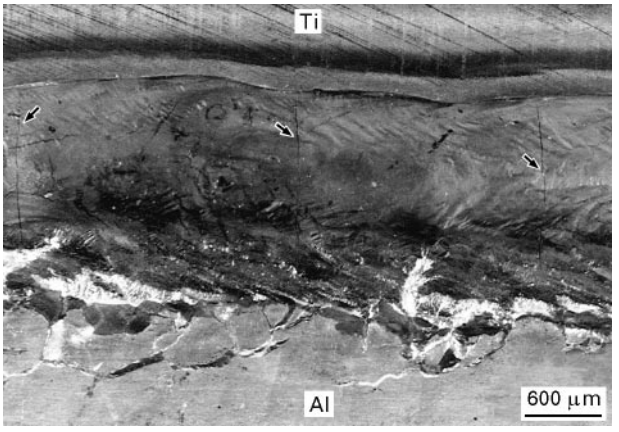

Figure 5 The top surface of the specimen welded at a speed of 1.00 m min^{-1} and an incident laser power of 2.0 kW, showing a transgranular crack. Arrows indicate the position of cracks.

3.2. Addition of Nb plates between Ti and Al alloys

The above experiments show that the crack free weld between Ti–6 wt% Al–4 wt% V and Al–1 wt% Mg–0.9 wt% Si is almost impossible to obtain by using a cw-CO_2 laser. The experiments are also performed on the joining of pure Ti and Al. The cracks are also found in the fusion zone and it is not possible to restrict the Al content below 20 at%. In order to prevent the mixing of Al in Ti alloy, it is necessary to put a barrier material between them. In the present study, a Nb plate is taken into consideration because of the following factors:

1. Nb melts at 2467 °C which is very high as compared to the melting point of Ti and Al [11].
2. Nb and Ti form a complete solid solution throughout the range of composition [6].
3. Nb increases the toughness of the Ti_3Al and TiAl intermetallic phases which form in the fusion zone [15].

Fig. 6a shows the microstructure of the sample that is welded with Nb plate (thickness, 0.6 mm) placed between Ti alloy and Al alloy. The laser offset is between Ti and Nb. It is interesting to note that no crack is observed in the fusion zone. Nb melts partially from the two sides of the plate. The corresponding concentration profiles are shown in Fig. 6b. The average Al content in the fusion zone is 11 at% which is within the range of Ti solid solution according to the phase diagram [6]. Nb also partially dissolves in the fusion zone, leading to the formation of Ti solid solution. The high-magnification microstructure around the interface (Fig. 6c) between the Nb plate and the Al alloy reveals that it consists of Al_3Nb globular particles in an Al matrix.

Fig. 7 shows the microstructure at the interface between the fusion zone and Al alloy where the Nb plate is melted completely. The average Al content in the fusion zone is 27 at% which is within the region of the Ti_3Al intermetallic phase according to the phase diagram [6]. One can observe the reappearance of a surface crack near the weld–Al alloy interface. In this case, the laser is exactly on the Nb plate resulting in the melting of more Al and dissolving it in the weld. When Nb wire is used instead of the plate, it is also found that the fusion zone consists of many cracks.

3.3. Mechanical properties

A comparison of the mechanical properties between the joint with and without a Nb plate is presented in this section. Fig. 8a and b shows the hardness profiles of the fusion zone for the specimen without and with a Nb plate, respectively. In Fig. 8a, one can observe a sharp increase in Vickers hardness up to 600 HV in the fusion zone immediately after the Ti side of the interface and it remains almost constant. The drop in hardness values is observed near the crack because of the stress relaxation. The results on hardness profile measurements are complemented with the concentration profiles in all experiments. It is observed that average Vickers hardness values increase to 700 HV on decrease in the Al content. When a Nb plate is added, one observes a flat hardness profile along the Ti alloy (Fig. 8b). The corresponding concentration profiles are shown in Fig. 6b. In this case, the hardness of the fusion zone does not increase with increasing Nb content.

Table II shows the tensile strengths of various samples tested with and without the addition of a Nb plate. One can observe that the values of strength for the samples with a Nb plate are very high compared with those of the samples without a Nb plate. It is to

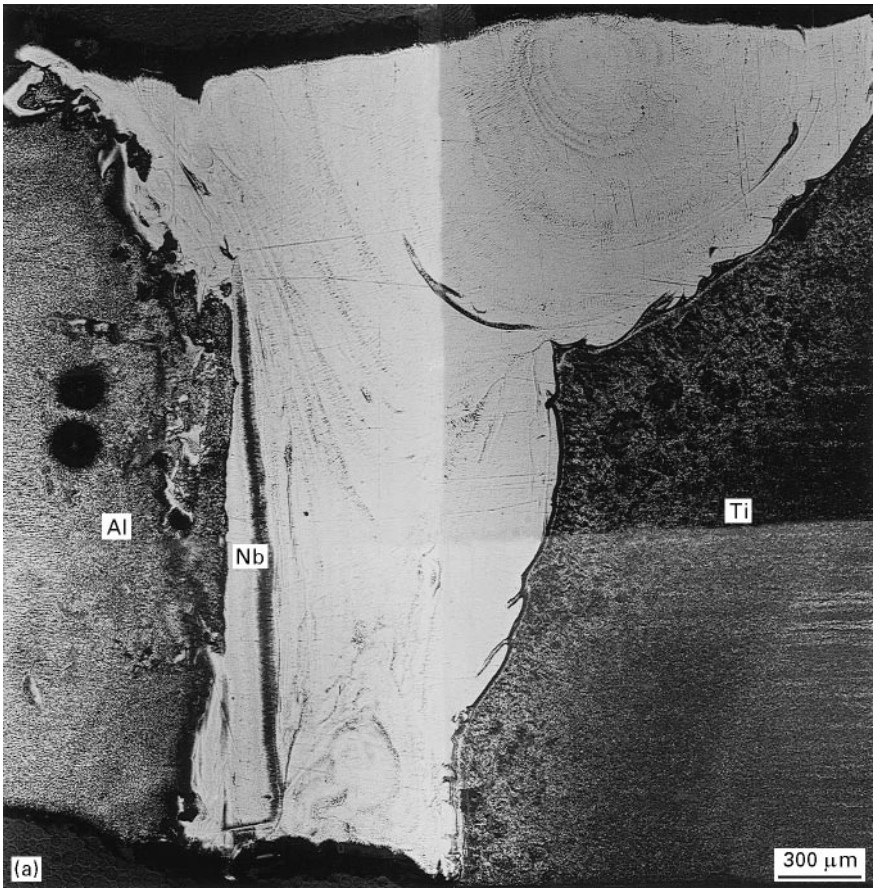

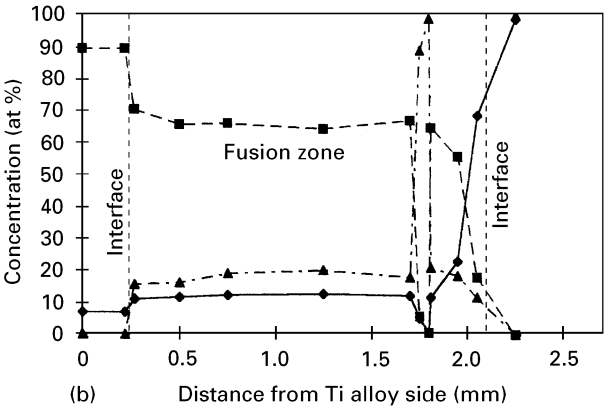

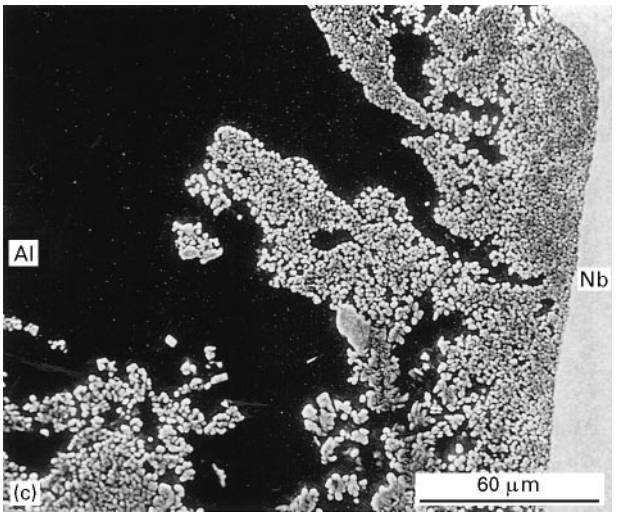

Figure 6 (a) Cross-section of the specimen welded at a speed of 1.00 mm min^{-1} and an incident power of 2.0 kW with the addition of a Nb plate sandwiched between the Ti alloy and the Al alloy showing the crack-free joint. The Nb plate melts partially from both sides. (b) Concentration profiles ((—◆—), Al; (– –■– –), Ti; (–·–▲–·–) Nb) of the same sample (laser offset on Ti–Nb interface). (c) High-magnification micrograph of the same sample at the interface region between Al and Nb, revealing the Al_3Nb globular precipitate in an Al matrix.

be noted that the true value of the tensile strength is not reflected because of the flaws in the weld. There exists a wide fluctuation in the results owing to the different dimensions of cracks and porosity. It is observed that, during tensile testing, failure in the Ti–Al joint occurs from the pre-existing crack in the fusion zone. In the case of samples with a Nb plate, failure takes place along the interface between the resolidified Al alloy and Nb plate. Fig. 9a shows the fracture surface of the tensile test specimen without Nb. One observes a transgranular cleavage fracture for the Ti–Al joint. In the case of the joint with a Nb plate (Fig. 9b), the fracture surface shows the presence of porosity at the interface between the Al alloy and the Nb plate. The inset is a high-magnification fractograph, revealing an intergranular mode of fracture. The composition analysis reveals that the particles are Al_3Nb.

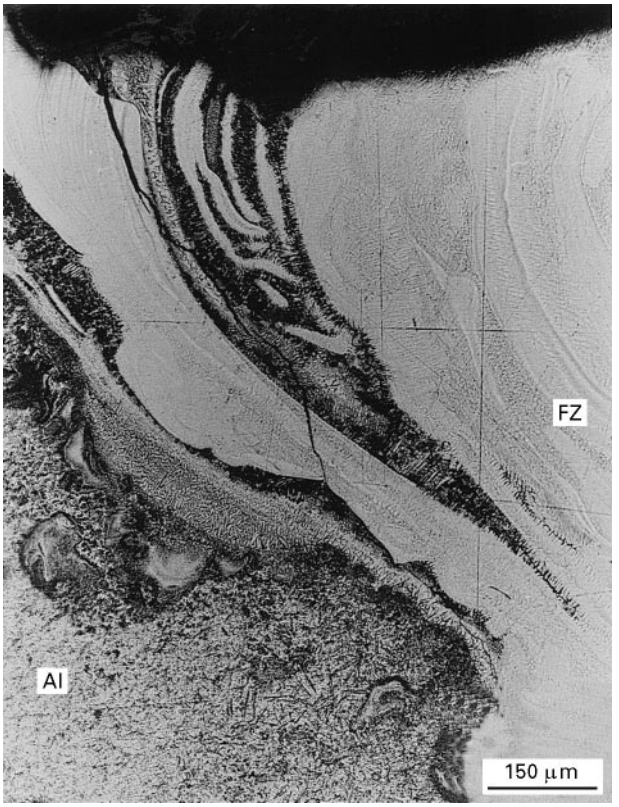

Figure 7 Cross section of the specimen welded at a speed of 1.00 mm min^{-1} and an incident power of 2.0 kW with the addition of a Nb plate sandwiched between the Ti alloy and Al alloy, showing the reappearance of the crack at the surface and that the Nb plate melts completely: FZ, fusion zone.

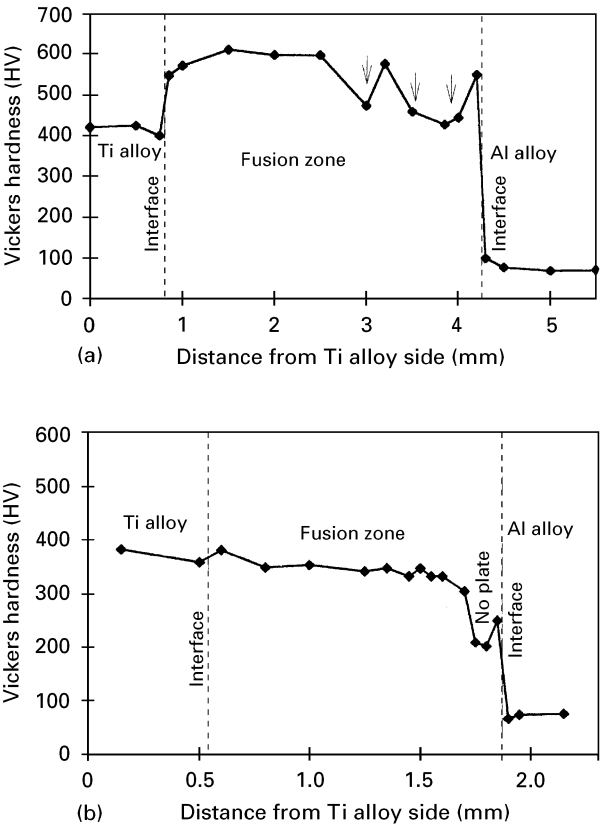

Figure 8 (a) Hardness profile of the specimen welded at a speed of 0.50 mm min^{-1} and an incident power of 2.0 kW (laser offset on the Ti alloy side). Arrows indicate the position of cracks. (b) Hardness profile of the specimen welded at a speed of 1.0 mm min^{-1} and an incident power of 2.0 kW with the addition of a Nb plate between the Ti alloy and Al alloy (laser offset on Ti–Nb interface).

4. Discussion

In the present investigation, an attempt has been made to identify the phases in the weld zone through an X-ray diffraction study. Unfortunately, the analysis cannot give any satisfactory results because insufficient area of the weld is available for the diffraction study. The combined results on the concentrations and hardness can give an idea of the possible formation of the phases in the fusion zone. There exists a uniform average composition in the fusion zone. The range of compositions indicates that either Ti_3Al or TiAl or both intermetallics are present [6]. Again, the properties of these two intermetallics are such that both the room-temperature strength and toughness of Ti_3Al are more than that of TiAl [15]. Moreover the ductility of the Ti_3Al can be enhanced by retaining the β-phase if the cooling rate is high. Our results show that the hardness of the sample with lower Al content is high compared with that for the sample with high Al content. It is also observed that the crack intensity is less for the sample with low Al content. All these observations reveal that the low Al content favours the formation of the Ti_3Al phase whereas the TiAl phase is formed in the sample with high Al content. That is why the pronounced long crack can be observed in a sample where the formation of TiAl is favoured.

Cracks are formed owing to the development of high stress. As the intermetallic phases that are formed in the fusion zone have very little ductility [14], they cannot withstand the stress, and failure occurs. Cracks are always found near the Al side of the interface. The thermal conductivity of the Al alloy is 193 W m^{-1} K^{-1}, whereas that for the Ti–6 wt% Al–4 wt% V alloy is 5.8 W m^{-1} K^{-1} [11]. Intermetallic phases can have still lower values. This indicates that a very high thermal gradient exists across the interface between the fusion zone and the Al resolidified alloy. This causes a high stress near the interface, and the intermetallic phase cannot withstand this

TABLE II The values of tensile strength for the samples with and without a Nb plate

Sample	Type of joint	Tensile strength (MPa)
1	Ti–Al	33
2	Ti–Al	57
3	Ti–Nb(0.4 mm)–Al	74
4	Ti–Nb(0.4 mm)–Al	107
5	Ti–Nb(0.4 mm)–Al	127
6	Ti–Nb(0.4 mm)–Al	110
7	Ti–Nb(0.4 mm)–Al	117
8	Ti–Nb(0.7 mm)–Al	70
9	Ti–Nb(0.7 mm)–Al	120
10	Ti–Nb(0.7 mm)–Al	98

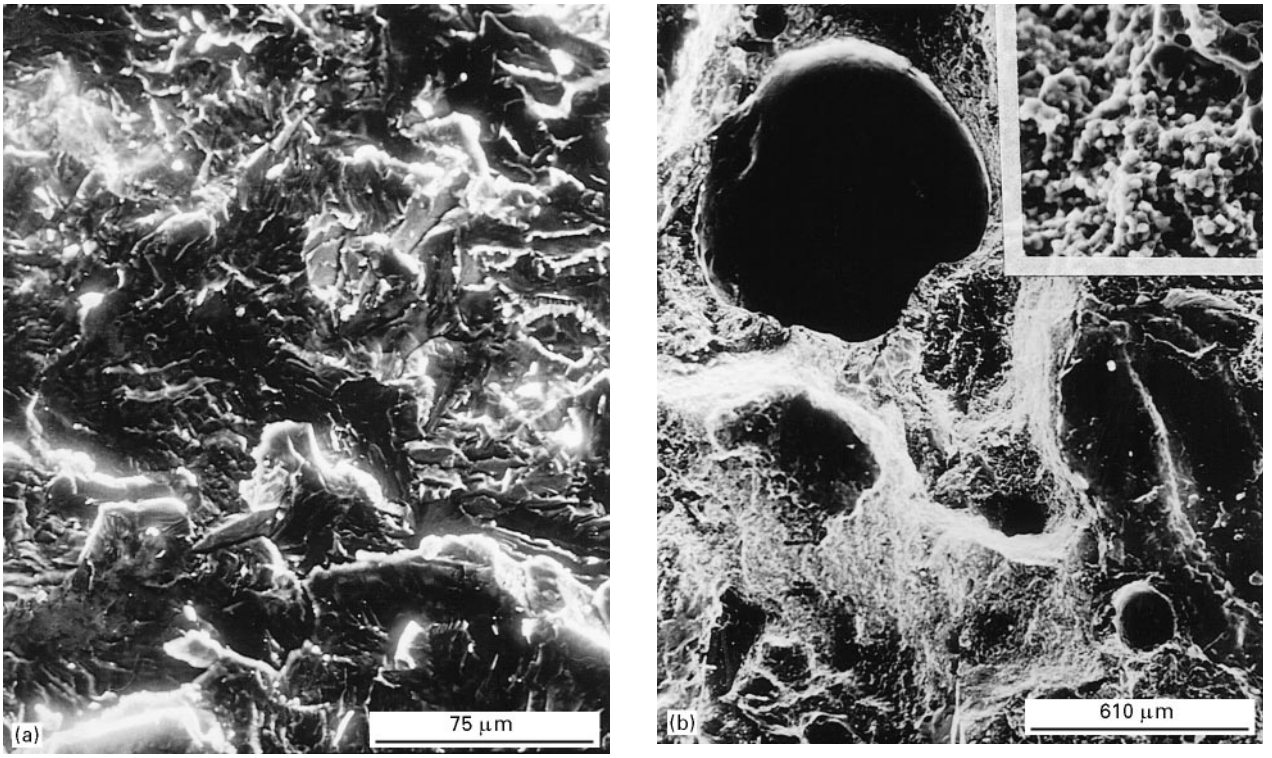

Figure 9 (a) Fractograph of the tensile test specimen without a Nb plate showing transgranular cleavage fracture. (b) Fractograph of the tensile test specimen with a Nb plate showing a large number of porosity at the interface between the Nb and the Al alloy. The inset shows a high-magnification fractograph indicating the intergranular mode of fracture.

thermal shock, resulting in the formation of cracks in this region. The increase in velocity also affects the thermal gradient, leading to the formation of more transverse cracks that can be seen in Fig. 5. In the case of other dissimilar joints [16], the cracks in the weld are mostly found close to the interface between the fusion zone and the parent metal that has a higher conductivity.

The composition cannot be restricted within the Ti solid solution range by any combination of laser parameters, although it is difficult to melt Al by a CO_2 laser [11]. The problem can be overcome when Nb is added between the Ti alloy and Al alloy. The optimum condition should be maintained to restrict the melting of the Nb plate from both sides of the plate is such a way that part of the material would dissolve in the Ti alloy and Al alloy individually. In this case, no intermetallic phase can be formed as very little Al can be dissolved in the fusion zone and it consists of Ti-rich solid solution. There is no change in hardness values observed in the fusion zone compared with the hardness of the Ti alloy. This means that the presence of Nb in Ti alloy acts only as a toughening agent. Thus, the fusion zone can have enough capability to be deformed by the stress developed during cooling. This leads to the formation of a crack-free weld. The fractograph in Fig. 9b shows that the failure between the Nb plate and Al alloy region occurs because of the porosity and the grain-boundary weakness. This is once again the failure of the Al alloy remelted zone, instead of the weld.

5. Conclusions

The following conclusions can be drawn from the present study.

1. In the case when Ti alloy and Al alloy are joined, the cracks are formed in the fusion zone because the intermetallic phases (TiAl and Ti_3Al) that have formed have almost no ductility to withstand the thermal stresses.
2. Cracks are always found near the Al side of the interface. Al, having a very high thermal conductivity, extracts heat readily and this causes a very high thermal gradient across the interface.
3. The dissolution of Al in the weld pool cannot be restricted within the range of the Ti solid solution.
4. The addition of a Nb plate serves as a barrier material to dissolve Al into the weld pool. In this case, the strength of the joint is very high compared with the joint without a Nb plate that contains flaws.
5. During tensile testing, the fracture occurs from the pre-existing cracks in the case of the joint without a Nb plate whereas, in case of the joint with a Nb plate, the fracture occurs at the interface between the Al resolidified zone and the Nb plate.

Acknowledgement

One of the authors (B. Majumdar) would like to acknowledge DLR for providing the fellowship through Indo-German bilateral co-operation programme for a period of one year.

References

1. A. M. GREEN and R. R. IRVING, *Iron Age*, April 30, (1970) 68.
2. A. A. OSOKIN, *Weld. Prod.* **23** (1976) 14.
3. V. D. SAPRYGIN, *ibid.* **22** (1975) 21.

4. G. CAM, D. DOBI, M. KOCAK, L. HEIKINHEIMO and M. SIREN, GKSS – Forschungszentrum, GKSS 95/E/23 (1995) p. 233.
5. L. V. LANKINA and YU. M. KORENYUK, *Weld Prod.* **21** (1974) 4.
6. T. B. Massalski (ed.) "Binary alloy phase diagrams" (American Society for Metals, Metals Park, OH, 1986).
7. R. HULTGREN, P. DESAI, D. HAWKINS, M. GLIESER and K. KELLEY, in "Selected values of thermodynamic properties of the binary systems " edited by R. Hultgren (American Society for Metals, Metals Park, OH, 1973).
8. G. SAUTHOFF, *Mater. Sci. Technol.* **8** (1996) 676.
9. J. MAZUMDAR, *J. Metals* **34** (1982) 16.
10. Z. SUN and J. C. ION, *J. Mater. Sci.* **30** (1995) 4204.
11. E. A. Brandes, (ed.) in "Smithells" metals reference handbook (Butterworths, London, 1983).
12. J. SERETSKY and E.R. RYBA, *Welding Journal*, 55(7), 1976, Welding Research Supplement 208-s.
13. P. S. LIU, W. A. BAESLACK III and J. HURLEY, *Welding Journal*, 73(7), 1994, Welding Research Supplement 175-s.
14. C. Dawes, (ed.) in "Laser welding—a practical guide" (Abington Publishing, Cambridge Cambs. 1992) p. 64.
15. F. H. FROES, C. SURYANARAYANA and D. ELIEZER, *J. Mater. Sci.* **27** (1992) 5113.
16. G. METZGER and R. LISON, *Welding Journal*, 55(8), 1976, Welding Research Supplement 230-s.

Received 26 March
and accepted 29 May 1997